Probing Majorana neutrinos in the normal mass hierarchy with TPCs

Zixin Chen*

(Dated: 1 December 2020)

Abstract: In this report, we evaluate the design of a detector for searching the neutrinoless double-β decay in the normal mass regime with a target half-life sensitivity of approximately 10^{30} years using time projection chambers. It is found that a kiloton scale gas-phase detector is capable of achieving the target sensitivity within an exposure of 10 years, and the dominant backgrounds for such a detector mainly result from the internal two-neutrino double-β decays. A good energy resolution and background rejection efficiency is crucial for achieving the target sensitivity.

CONTENTS

I. INTRODUCTION

Neutrinoless double-β decay ($0\nu\beta\beta$) is a hypothetical mode of double-β decay which can only happen if neutrinos are Majorana fermions. The discovery of $0\nu\beta\beta$ would directly demonstrate a process beyond the Standard Model of physics violating the conservation of lepton number and provide further constraints on the mass of neutrinos [1]. However, the observation of $0\nu\beta\beta$ is rather difficult due to its exceptionally long half-life and susceptibility to various potential backgrounds [2]. Currently, the most stringent limit on $0\nu\beta\beta$ (in ^{136}Xe) is $T^{0\nu}_{1/2} > 1.07\times10^{26}$ yr at 90% C.L. [3] and future detectors that can probe the inverse hierarchy regime with a target half-life sensitivity of $T^{0\nu}_{1/2} \sim 10^{28}$ yr has been proposed [4]. But the current evidence from neutrino oscillations favors the normal hierarchy [5] and we should consider the design and implementation of detectors that would be able to probe this regime with a target sensitivity of $T^{0\nu}_{1/2} \sim 10^{30}$ yr.

Therefore, in this report, we investigate the possibility of probing Majorana neutrinos in the normal mass hierarchy using time projection chambers (TPCs). ^{136}Xe is chosen as the decay source and the scintillator. We first estimate the overall mass of the detector. Based on this estimation, we further evaluate the backgrounds, energy resolution, and sensitivity of such a detector. Finally, we end with some brief comments on the detector design and our calculations.

II. DETECTOR MASS

Under the hypothesis that only the known three light neutrinos participate in the decay process, the half-life formula for $0\nu\beta\beta$ is

$$\left(T^{0\nu}_{1/2}\right)^{-1} = G^{0\nu}\cdot|M^{0\nu}|^2\cdot\frac{|m_{\beta\beta}|^2}{m_e^2} \tag{1}$$

, where $|m_{\beta\beta}|$ is the effective Majorana mass, $G^{0\nu}$ is the phase space factor, $|M^{0\nu}|$ is the nuclear matrix element, and m_e is the electron mass. As shown below, the $|m_{\beta\beta}|$ is a linear combinations of the three neutrino mass eigenstates via the PMNS matrix,

$$m_{\beta\beta} = \left|\sum_i U^2_{ei}\cdot m_{\nu_i}\right| \tag{2}$$

where m_{ν_i} are the neutrino mass eigenvalues and U_{ei} is the mixing matrix elements. However, due to uncertainties in the absolute neutrino mass scale and PMNS matrix elements, the allowed parameter space of $|m_{\beta\beta}|$ spans till 10^{-5} eV.

From the corresponding coverage regions in Figure (1), we see that for $|m_{\beta\beta}|$ around 10^{-3} eV, there is more than 95% probability for the detection of a $0\nu\beta\beta$ signal. Given the high probability and the practical limitations on Xenon supply, we choose $|m_{\beta\beta}| = 10^{-3}$ eV and estimate a target half-life of $T^{0\nu}_{1/2} \sim 8.72\times10^{29}$ yr using the values in Table (1). With this half-life, we require a decay rate of 1 event/yr in our detector, which yields $\sim$ 298 ton ^{136}Xe for the active mass. In the rest of the

* Yale College, Class of 2023.5, email: zixin.chen@yale.edu

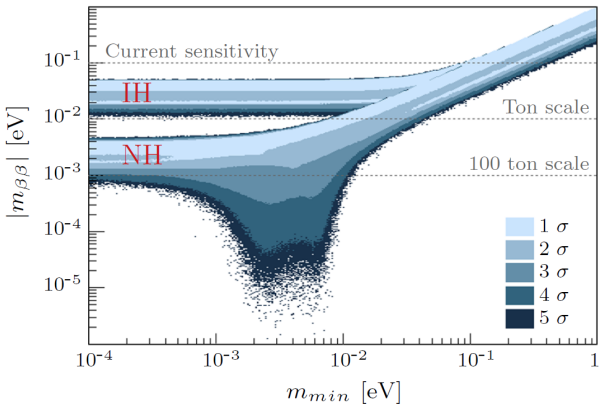

FIG. 1. Allowed parameter space for $m_{\beta\beta}$ [6]

paper, we round this number up to 0.3 kiloton and use 0.5 kiloton total mass to estimate the size of the detector.

$G^{0\nu}$	$M^{0\nu}$	m_e	^{136}Xe atomic mass
10^{-14} yr	(avg)	MeV	Da
3.56	2.9	0.511	135.91

TABLE I. Table of values for $T^{0\nu}_{1/2}$ and ^{136}Xe total mass estimation

III. BACKGROUNDS

With a Q-value of $Q_{\beta\beta} = 2458.07 \pm 0.31$ keV, ^{136}Xe $0\nu\beta\beta$ is subject to multiple backgrounds. For the existing $0\nu\beta\beta$ TPC detectors, the dominant backgrounds include: (i) charged current (CC) and neutral current (NC) interactions from solar neutrinos (ii) ^{136}Xe two-neutrino double-β decay ($2\nu\beta\beta$) (iii) long-lived radionuclides from ^{238}U and ^{232}Th natural decay chains (iv) neutron captures on ^{136}Xe and the subsequent β decays from ^{137}Xe.

It can be shown that (i) and (ii) are the dominant backgrounds for a kiloton scale detector. Therefore, We will examine (i) and (ii) numerically, and briefly introduce the veto-systems that render (iii) and (iv) negligible.

A. Neutrino-induced backgrounds

Making up approximately 0.3% of the known matters in our universe, neutrinos are abundant particles that can interact both with the nuclei and orbiting electrons of ^{136}Xe. More specifically, electron neutrinos with sub-MeV energies and above can interact with the ^{136}Xe nuclei via either CC interactions or NC elastic scattering off electrons to produce backgrounds near the region of interest (ROI). The interactions are shown in Equation (3) and (4), and no inelastic scattering produces backgrounds of interest has been found.

$$\nu_e + e^- \rightarrow \nu_e + e^- \tag{3}$$

$$\nu_e + {}^{136}\mathrm{Xe} \rightarrow e^- + {}^{136}\mathrm{Cs} \tag{4}$$

Figure (2) shows different sources of neutrino fluxes reaching the earth. Obviously, the majority of neutrinos that will generate the backgrounds mentioned above are solar neutrinos. We use the solar neutrino flux spectra in Figure (3) to estimate the neutrino-induced backgrounds.

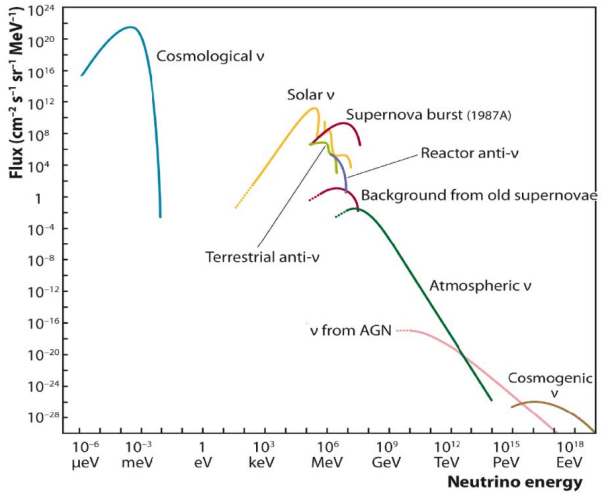

FIG. 2. Neutrino flux verses energy for various sources

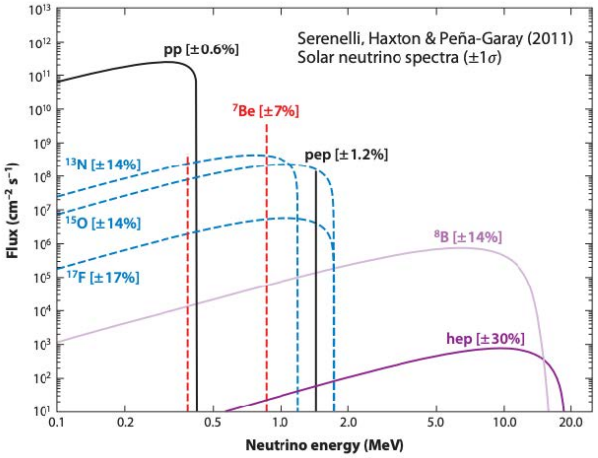

FIG. 3. Solar Neutrino Flux Spectra [7]

1. *Charged Current Interaction*

Three possible backgrounds can originate from the CC interaction [8]: (a) The product ^{136}Cs may undergo β decays and emit e^- with γ rays, the total energy of which

may populate the $0\nu\beta\beta$ ROI. (b) CC captures can produce ^{136}Cs either in its ground state or one of its excited states. If ^{136}Cs is in an excited state below the particle emission threshold, it will emit γ rays and relax back into its ground state. The total energy of the γ rays together with the e^- from CC interactions may produce a spectrum that surpasses the $0\nu\beta\beta$ Q-value. (c) If ^{136}Cs is produced in an excited state above the particle emission threshold, then the emissions of a p or n may follow, along with radiation from the resultant nucleus. e^-, p or n, and the additional radiation together constitute potential backgrounds. It has been shown in [8] that (b) and (c) are negligible compared to (a). Thus, we only examine the ^{136}Cs β decays from the CC interactions.

Calculating the ^{136}Cs production rate is equivalent to calculating the CC capture rate. We use the cross section of CC capture given by

$$\begin{aligned}\sigma_k &= \frac{G_F^2\cos^2\theta_c}{\pi} p_e E_e F(Z,E_e)\left[B(F)_k + \left(\frac{g_A}{g_V}\right)^2 B(GT)_k\right] \\ &= (1.597\times10^{-44}\text{cm}^2) p_e E_e F(Z,E_e) \\ &\times \left[B(F)_k + \left(\frac{g_A}{g_V}\right)^2 B(GT)_k\right] \end{aligned} \quad (5)$$

and the survival probability of solar electron neutrinos as

$$P_{E_\nu} = 0.336 + 0.117e^{\frac{-E_\nu-0.1}{4.82}} + 0.119e^{\frac{-E_\nu-0.1}{4.88}} \quad (6)$$

to compute the rate of captures via the following integral.

$$R = \sum_k \int \sigma_k(E_\nu)\frac{d\phi_\nu}{dE_\nu} P_{E_\nu} dE_\nu \quad (7)$$

Here, p_e, E_e are the outgoing electron momentum and energy respectively. $F(Z,E_e)$ is the Fermi function. $B(F)_k, B(GT)_k$ are the Fermi response and the Gamow-Teller response. g_A, g_V are axial vectors. The constant in Equation (5) is applicable for neutrinos with MeV energies [8]. $\frac{d\phi_\nu}{dE_\nu}$ is the energy dependent flux for a specific type of neutrinos.

The energy threshold for CC capture on ^{136}Xe is ~ 0.59 MeV [9]. From Figure (3), we can see that ^{7}Be will be the dominant neutrinos contributing to CC captures, with a spectrum peak at 0.86 MeV at least $\sim 10^2\times$ higher than the other neutrino fluxes. The leading order of CC capture rates can be obtained with the ^{7}Be peak at 0.86 MeV alone. Using the values in Table (2) and digitized flux spectrum, we estimate $R \sim 6.47\times10^{-35}$ [per atom per second]. This is within a factor of 1.27 difference with the estimation in [8].

The energy spectrum of ^{136}Cs β decay from the product β and the promptly emitted γ is shown in Figure (4). Due to the complexity of ^{136}Cs β decay, we cite this spectrum and an estimated background rate for 0.2% FWHM of ~ 0.06 [events/(ton $\cdot$ yr)] directly from [8]. As shown in Figure (4), the variation of the Cs β decay event rate near the $0\nu\beta\beta$ ROI is negligible. Thus, we will scale this background rate for different energy resolutions.

$F(Z,E_e)$	g_A/g_V	$B(GT)$ 0.85 MeV	E_e MeV
8.87	1.267	0.082	1.38

TABLE II. Table of values for σ_k estimation. $B(F)$ is taken to be 0 because ^{7}Be strongly excites the low-lying 1^+ states. p_e is not listed, but could be easily estimated by p_e^2/m_e given that E_e is far below the relativistic limit.

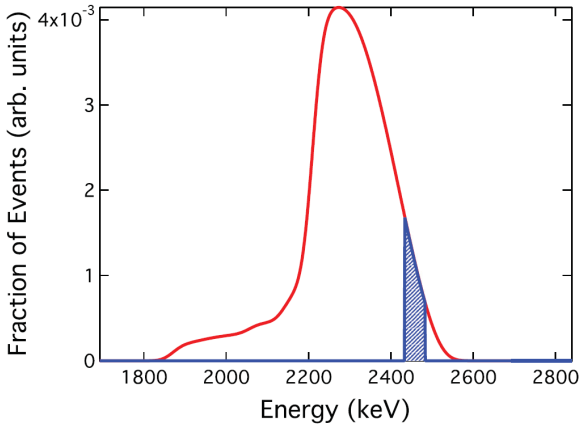

FIG. 4. The approximate $\beta-\gamma$ energy spectrum for ^{136}Cs decays. Shaded region is over the 0.2% FWHM interval at $0\nu\beta\beta$ Q-value. [8]

2. *Neutral Current Interaction*

For NC interactions, only neutrinos with energies near the $Q_{\beta\beta}$ will produce an outgoing electron with kinetic energy in the $0\nu\beta\beta$ ROI and constitute backgrounds. Figure (3) shows that only ^{8}B and hep neutrinos have energies near $Q_{\beta\beta}$, and heps are negligible compared to ^{8}B. Following a similar procedure in the CC background estimation, we use the cross section for $\nu-e^-$ scattering [10]

$$\begin{aligned}\frac{d\sigma}{dT} &= \frac{2G_F^2 m_e}{\pi} \\ &\times \left[g_L^2 + g_R^2\left(1-\frac{T}{E_\nu}\right)^2 - g_L g_R \frac{m_e T}{E_\nu}\right] \end{aligned} \quad (8)$$

and the survival probability as before to calculate the integral of the interaction rate below,

$$R' = \int_{2.4}^{2.5} \frac{d\sigma}{dT} P_{E_\nu} \frac{d\phi'}{dE_\nu} dE_\nu \quad (9)$$

where T is the kinetic energy of the recoiling electron, and other useful values are listed in Table (3). Neutrino fluxes are digitized from the ^{8}B neutrino spectrum. The background rate in the $2.4-2.5$ MeV energy window is plotted in Figure (5).

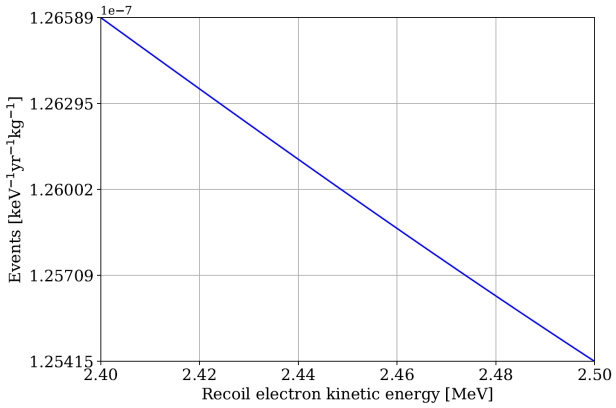

FIG. 5. Estimated NC interaction rate versus recoil electron kinetic energy

G_F [GeV^{-2}]	g_L	g_R	$\sin^2\theta_W$
1.17×10^{-5}	$\pm\frac{1}{2} + \sin^2\theta_W$	$\sin^2\theta_W$	0.23

TABLE III. Table of values for $d\sigma/dT$ estimation

B. Two neutrino double beta decay

In $0\nu\beta\beta$, since all decay energy is emitted via e^-, the energy spectrum has a distinct peak at the Q-value. This is very different from the $2\nu\beta\beta$ energy spectrum, which has a much wider energy window. Although the spectrum of 0ν and 2ν decays are very different, there will still be a tail from the 2ν broad spectrum extending into the 0ν peak, and because 0ν decays are too rare, the relative amplitude of its peak can get smeared over by that of the 2ν spectrum tail. Especially in our case, the 0ν peak can be around $8-9$ times smaller than that of the 2ν energy spectrum.

A good energy resolution is required to prevent the signal getting smeared over. In Figure (6), we show a relationship between the $2\nu\beta\beta$ background rate and the energy resolution from the EXO collaboration. At the 0.5% FWHM, the background rate is $\sim 10^{-4}$ [events/(ton $\cdot$ yr)].

C. Other backgrounds and veto systems

The long-lived radionuclides from ^{238}U and ^{232}Th natural decay chains that can contribute to the backgrounds mainly exist in the detector materials or result from the steady-state gaseous ^{222}Rn, which can infiltrate into the fiducial volume of the detector. For a kiloton scale $0\nu\beta\beta$ detector, the background γ or β from detector walls will effectively die out after some meters and can be ignored in the fiducial volume. The steady-state ^{222}Rn could be a potential problem. However, the actual contribution to the background comes from the subsequent ^{214}Bi β decay. It can be tagged by the α decay of ^{214}Po immediately after it. The efficiency of the ^{214}Bi-Po α tag is shown to be $\geq 99\%$ in [11].

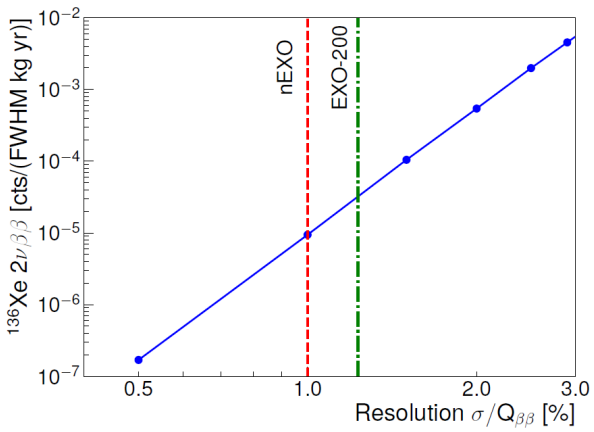

FIG. 6. ^{136}Xe $2\nu\beta\beta$ event rate versus the energy resolution. The expected and measured energy resolution of nEXO and EXO-200 are also shown for reference. [4]

Neutrons from various sources can get captured on ^{136}Xe and the subsequent β decays from the resulting ^{137}Xe present a potential background. However, it has been shown in [12] that this background can be veto-ed with high efficiency for a kiloton scale detector via the cascade of γ rays with Q value 4025.5 ± 0.3 keV upon thermal neutron captures [13].

IV. SENSITIVITY AND DISCOVERY POTENTIAL

With the detector mass and the dominant background rates, we calculate the sensitivity and the discovery potential versus exposure for different background rates. As shown in Figure (7), for an exposure of 3 [kiloton $\cdot$ yr], we can achieve our target sensitivity with at most an averaged rate of ~ 3 background events per year. Meanwhile, the estimated raw background rate with 0.1% FWHM energy resolution is ~ 9.21 [cts/(0.3 kiloton $\cdot$ yr)]. This seems to have failed in achieving our goal even with some very idealized estimations. However, most of the backgrounds are induced by neutrinos. Those backgrounds can be rejected with high efficiency using the topological discrimination of TPCs. In fact, the only background that will pose a problem is the ^{136}Xe $2\nu\beta\beta$. To prevent $2\nu\beta\beta$ backgrounds from smearing the $0\nu\beta\beta$ signals, we currently have no better alternatives than improving the energy resolution of the detector, since the experimental signature of $2\nu\beta\beta$ near the ROI is very similar with that of the $0\nu\beta\beta$: both are detected as two e^- with total kinetic energy near the $Q_{\beta\beta}$. Sub-percent energy resolution will limit its rate to the order of ~ 0.1 [cts/yr], demonstrating good promise in detecting 0ν signals. In the next section, we elaborate on the energy resolution and topological discrimination of TPCs.

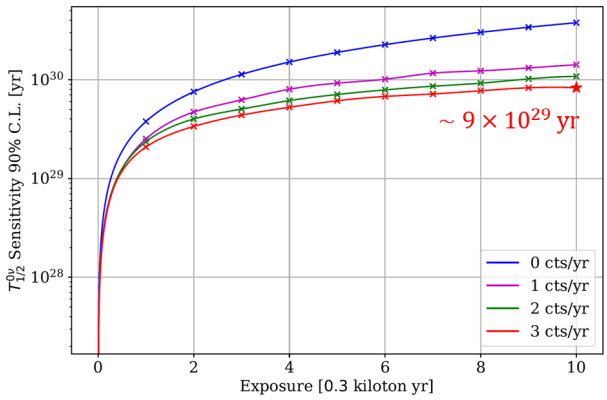

FIG. 7. Sensitivity versus exposure at 90% C.L.

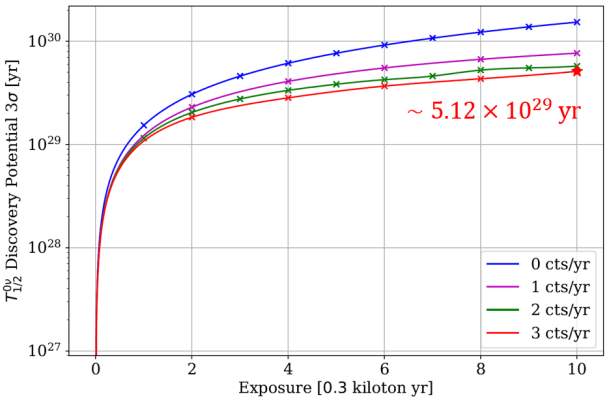

FIG. 8. 3σ discovery potential versus exposure

V. ENERGY RESOLUTION AND DETECTOR DESIGN

So far, the best energy resolution achieved in $0\nu\beta\beta$ TPC detectors is $\sim 0.5\%$ for high pressure gas Xe TPCs (HPgXeTPCs) [11]. For liquid Xe (LXe) TPCs, the best result from simulations predict an energy resolution $\sim 1\%$ [4]. As shown in Figure (9), gas Xe have better intrinsic energy resolution than LXe, and the electroluminescence conversion adopted in HPgXeTPC yields high gain with low noise [14]. Meanwhile, the relatively low light collection efficiency in LXe TPCs poses a challenge in further improvements of energy resolution. Moreover, HPgXeTPCs like NEXT-100 have demonstrated topological discrimination from track reconstructions. This enables HPgXeTPCs to reject backgrounds better than LXe TPCs, which are using single-site (SS) and multi-site (MS) selections. Although SS-MS discrimination can effectively reject γ rays from MS scatterings, track reconstructions can also reject SS β decays very well based on the number of Bragg peaks. The above mentioned neutrino backgrounds from ^{136}Cs β decays and NC scatterings can therefore be rejected with high efficiency in HPgXeTPCs. With a better energy resolution and background rejection method, HPgXeTPCs seem to be a reasonable choice for our purpose.

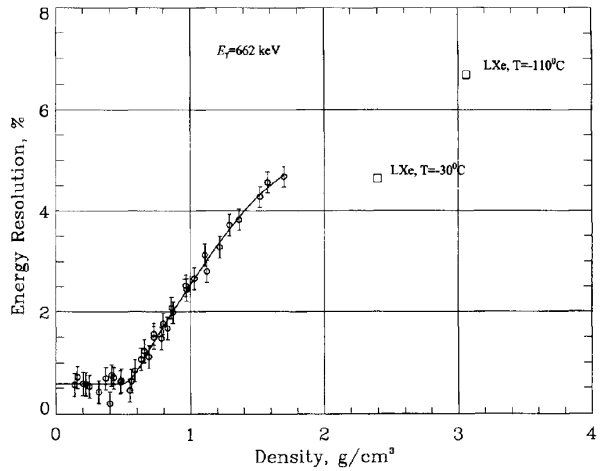

FIG. 9. Density dependencies of the intrinsic energy resolution in Xe measured for 662 keV γ rays [15]

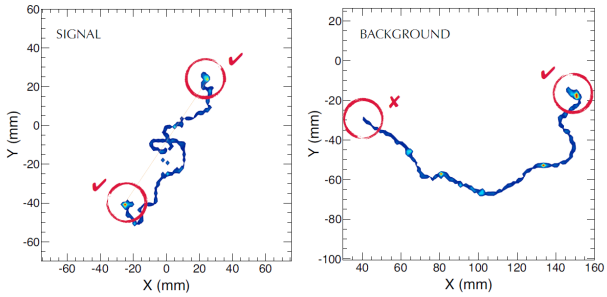

FIG. 10. Simulated trajectory for $\beta\beta$ (left) and β right) in Xe gas [11]

Finally, we estimate the size of our kiloton scale detector to complete our evaluations and perform a sanity check on the previous claim that γ and β from detector walls is negligible in the fiducial volume. The current HPgXeTPC designs have internal pressure up to 20 bar, and the Liquid-Vapor saturation gas density at 20 bar, 242.85K is ~ 0.1736 g/cm^3 [16]. With this density and a total mass of 0.5 kiloton, a cylindrical detector with height D and radius $\frac{D}{2}$ will have a radius of ~ 9.71 m. Thus, we will have a 10-meter scale detector and it can be verified that γ and β with energy around 2.5 MeV have penetration depth on the meter scale. Thus, they will not constitute dominant backgrounds in a kiloton scale detector.

VI. DISCUSSIONS AND OUTLOOK

Currently, the best limit on $0\nu\beta\beta$ half-life comes from the KamLAND-Zen experiment at $\sim 10^{26}$ years [3]. Although the detector had a relatively poor energy resolu-

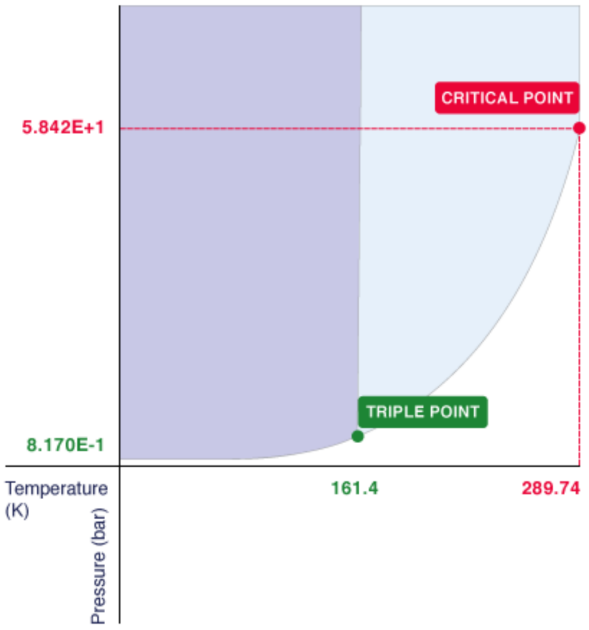

FIG. 11. Xe under solid (grey), liquid (blue) and vapor states (white) along the equilibrium curves [16]

tion, the collaboration compensated for it by employing 0.3 ton Xe. However, from our estimation, we see that at kiloton scale the backgrounds mainly come from neutrinos and 2ν decays. They cannot be reduced by simply having a bigger detector, but instead scale with it. Therefore, good energy resolution and background rejection efficiency should be considered for the next generation detectors. TPCs have the spatial reconstruction power that can reject most backgrounds except for some 2ν decays once coupled with a good energy resolution. This is essential for the success of the $0\nu\beta\beta$ search in the normal mass regime and provides a strong motivation for further investigations into the design of TPC-based $0\nu\beta\beta$ detectors for the normal mass regime.

We also note for completeness that many detector design details are ignored in this report, and the detector itself is very idealized. We therefore urge readers to take all estimations with a grain of salt and expect less perfect performance from a real-world detector.

VII. CONCLUSIONS

Our evaluation suggests that in order to probe $0\nu\beta\beta$ in the normal mass regime with TPCs, we will likely need a kiloton scale HPgXeTPC with sub-percent energy resolution and good topological discrimination. However, we do not rule out the feasibility of a LXe TPC for this task since it has similar performance and may avoid some technical issues faced by a kiloton scale HPgXeTPC.

At kiloton scale, most backgrounds come from neutrinos and $2\nu\beta\beta$. The topological discrimination power and sub-percent energy resolution makes HPgXeTPCs competitive candidates for the $0\nu\beta\beta$ search in the normal mass regime. If we can obtain enough ^{136}Xe for such a kiloton scale detector, it is optimistic that we will be able to perform such experiment with success.

ACKNOWLEDGMENTS

The author would like to thank Professor David Moore for guiding the general direction of the project and teaching her to think about the big picture, and TA Ako Jamil for advice on the details of some calculations.

[1] M. Fukugita and T. Yanagida, Barygenesis without grand unification, Physics Letters B **174**, 45 (1986).
[2] S. D. Biller, Probing majorana neutrinos in the regime of the normal mass hierarchy, Phys. Rev. D **87**, 071301 (2013).
[3] A. Gando and et al. (KamLAND-Zen Collaboration), Search for majorana neutrinos near the inverted mass hierarchy region with kamland-zen, Phys. Rev. Lett. **117**, 082503 (2016).
[4] J. B. Albert and et al., Sensitivity and discovery potential of the proposed nexo experiment to neutrinoless double- decay, Physical Review C **97**, 10.1103/physrevc.97.065503 (2018).
[5] K. Abe and et al., Constraint on the matter-antimatter symmetry-violating phase in neutrino oscillations (2019), arXiv:1910.03887 [hep-ex].
[6] G. Benato, Effective majorana mass and neutrinoless double beta decay, The European Physical Journal C **75**, 10.1140/epjc/s10052-015-3802-1 (2015).
[7] A. M. Serenelli, W. C. Haxton, and C. Peña-Garay, Solar models with accretion. i. application to the solar abundance problem, The Astrophysical Journal **743**, 24 (2011).
[8] H. Ejiri and S. R. Elliott, Charged current neutrino cross section for solar neutrinos, and background to $\beta\beta(0\nu)$ experiments, Phys. Rev. C **89**, 055501 (2014).
[9] S. Haselschwardt, B. Lenardo, P. Pirinen, and J. Suhonen, Solar neutrino detection in liquid xenon detectors via charged-current scattering to excited states, Physical Review D **102**, 10.1103/physrevd.102.072009 (2020).
[10] N. F. de Barros and K. Zuber, Solar neutrino–electron scattering as background limitation for double-beta decay, Journal of Physics G: Nuclear and Particle Physics **38**, 105201 (2011).
[11] J. Martín-Albo and et al., Sensitivity of next-100 to neutrinoless double beta decay, Journal of High Energy Physics **2016**, 10.1007/jhep05(2016)159 (2016).
[12] J. Albert and et al., Cosmogenic backgrounds to 0 in exo-200, Journal of Cosmology and Astroparticle Physics **2016** (04), 029–029.

[13] S. G. Prussin, R. G. Lanier, G. L. Struble, L. G. Mann, and S. M. Schoenung, Gamma rays from thermal neutron capture in ^{136}Xe, Phys. Rev. C **16**, 1001 (1977).

[14] D. Nygren, High-pressure xenon gas electroluminescent tpc for 0- -decay search, Nuclear Instruments and Methods in Physics Research Section A: Accelerators, Spectrometers, Detectors and Associated Equipment **603**, 337 (2009).

[15] A. Bolotnikov and B. Ramsey, The spectroscopic properties of high-pressure xenon, Nuclear Instruments and Methods in Physics Research Section A: Accelerators, Spectrometers, Detectors and Associated Equipment **396**, 360 (1997).

[16] A. liquide, Gas encyclopedia for xenon (2020).